Spectroscopy (Solid state physics)

I Electronic states

1) ①Single-electron (quasi-particle) energy of valence electrons, Band mapping :$E(\boldsymbol{k})$

② Occupation number: $3d^n$, $4f^n$

2) Repulsive energy between two electrons: U

3) Magnetic states: Spin moment: $\langle S_z \rangle$

Orbital moment: $\langle L_z \rangle$

II Experimental methods

1)*Photoabsorption spectroscopy*

2)Photoelectron (photoemission) spectroscopy

①Angle-resolved photoemission spectroscopy

②*Resonance photoemission spectroscopy*

3)*Magnetic circular dichroism*

4) Soft-X-ray Raman spectroscopy

2^{nd} order optical process,

giving more information than 1^{st} order optical processes

Photoemission Spectroscopy

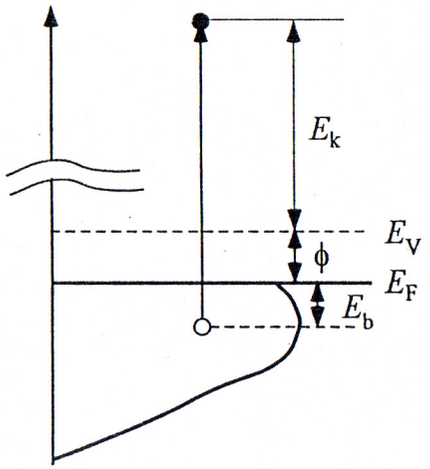

$$E_k = h\nu - \phi - E_b$$

1) Usually surface sensitive at lower photon energies

*Escape depth～1–2 nm

2) More bulk sensitive when hν> 200–400 eV

3) Energy resolution: ΔE> 5 meV

Angle-resolved photoemission

1) Needs single crystals

2) Needs high brightness

Resonance photoemission

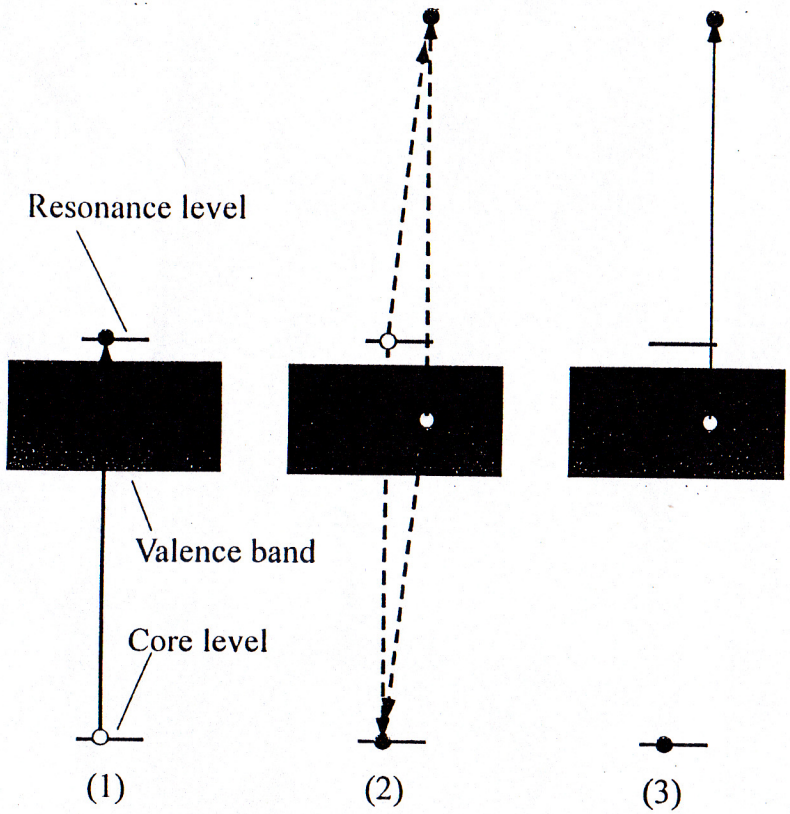

(2) and (3) : an identical state except the phase

(2) and (3) can interfere. *Fano profile*

Resonance occurs locally,

reflecting the local electronic states.

Constant initial state spectra (CIS)

Simultaneous scanning of the photon energy and the kinetic energy of photoelectrons detected

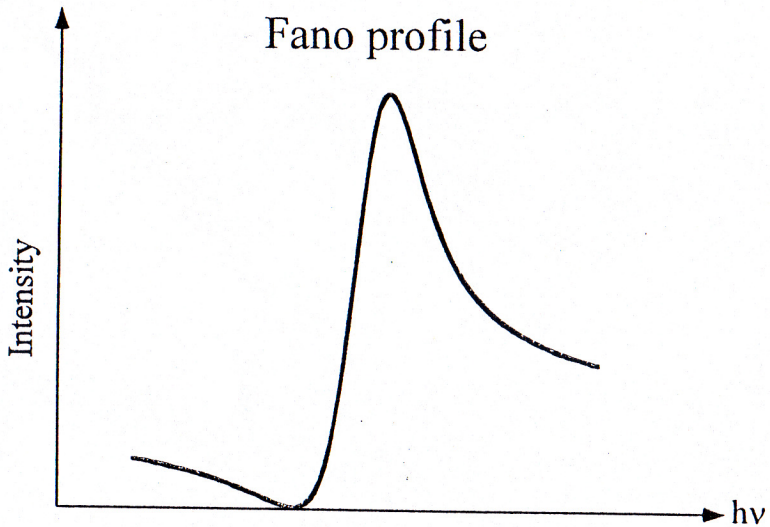

$$I(\varepsilon) = I_0 \frac{(q+\varepsilon)^2}{1+\varepsilon^2}, \quad \varepsilon = \frac{h\nu - h\nu_0}{\Gamma}$$

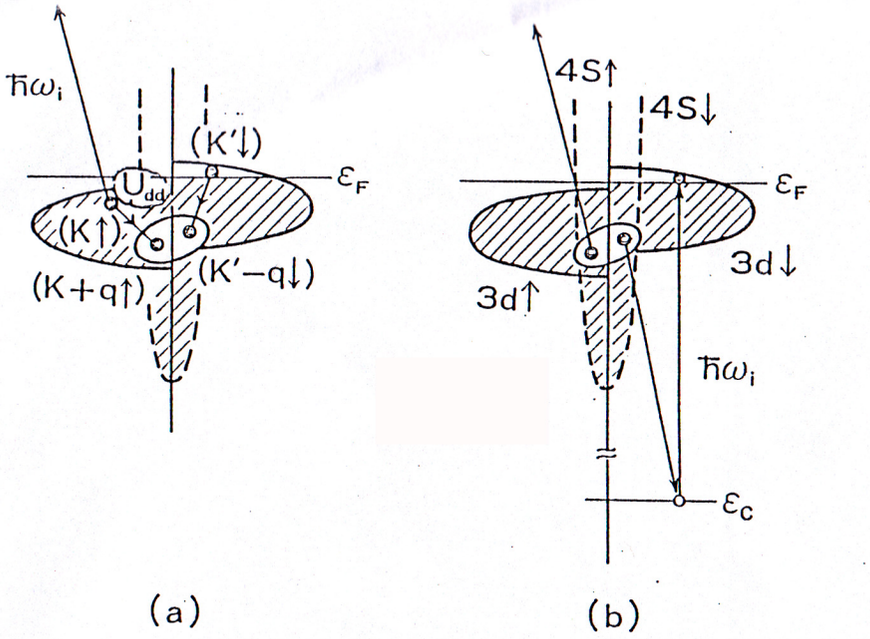

(a) (b)

Fig. 16

$\Delta E = \varepsilon_d + U_{dd}$

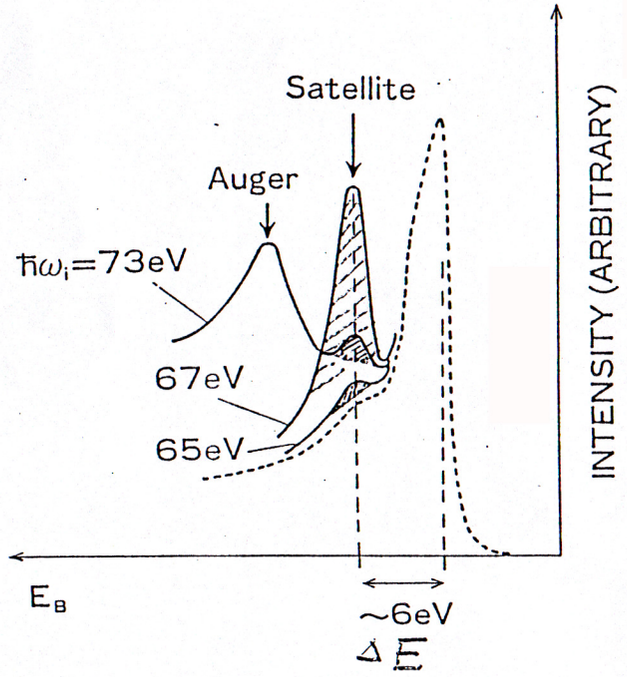

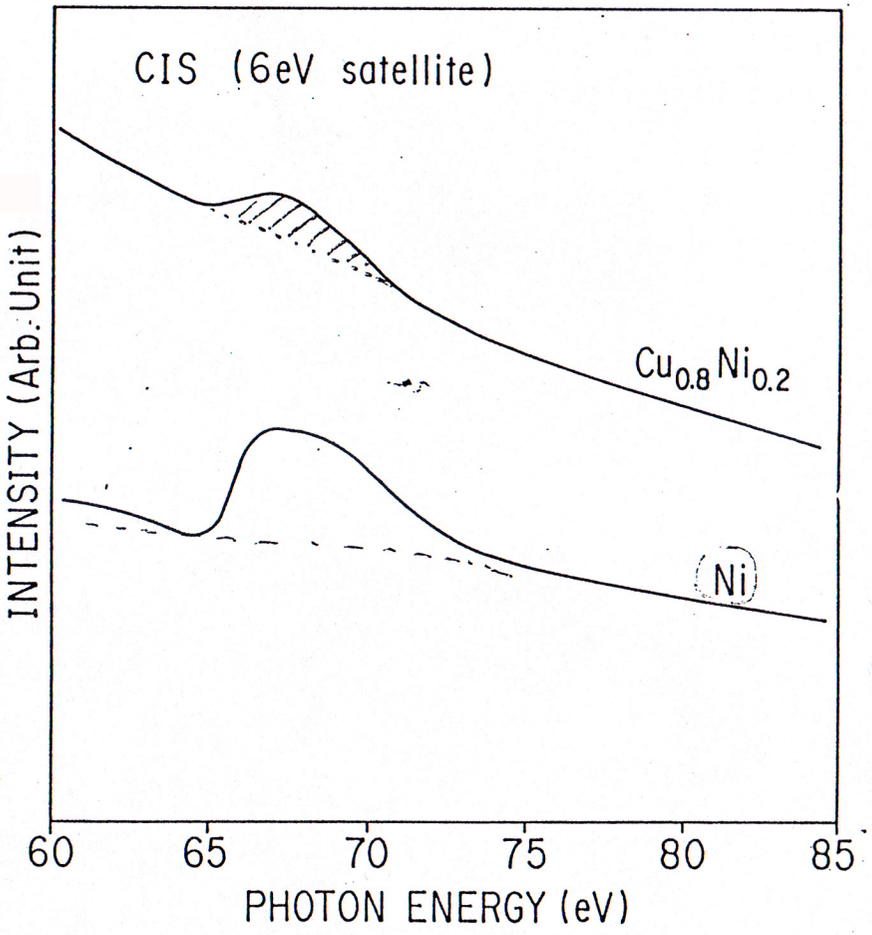

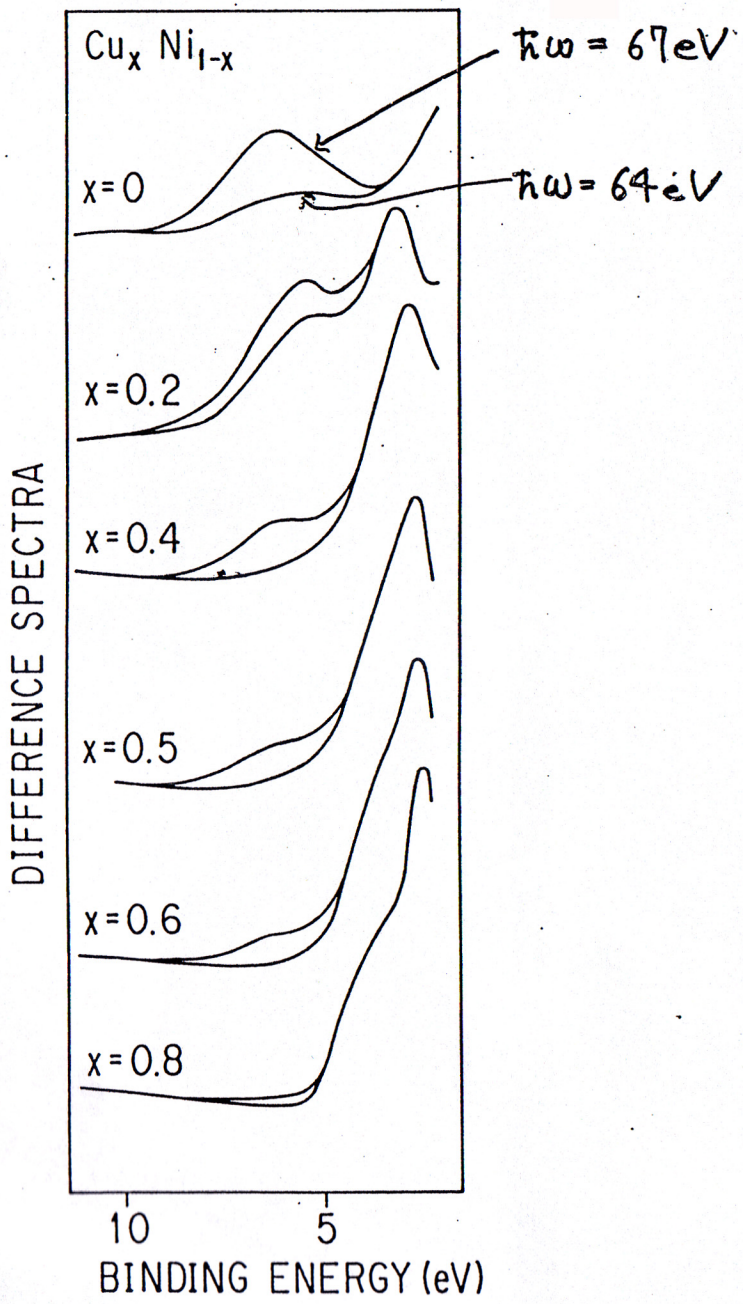

Response of many electron system to VUV and SX

1) Local excitation (Importance of core hole

[Initial state : localized
[final state : modified by surrounding

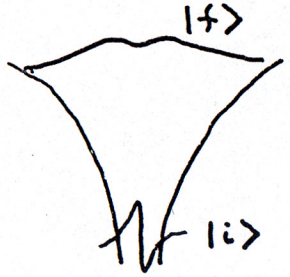

$\langle f|\hat{x}|i\rangle$

2) Rapidity of excitation

[excitation : $\Delta t \sim \omega^{-1} \sim \omega_{th}^{-1}$
[relaxation : $\tau \sim (\omega - \omega_{th})^{-1}$

$\Delta t \ll \tau \Rightarrow$ "Sudden approximation"

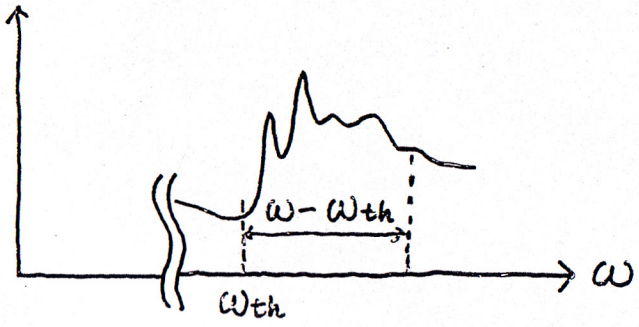

4'

Ce 4*d*-4*f* and Ce 3*d*-4*f* RPES of $CeRu_4Sb_{12}$

Ce 4*d*-4*f* Excitation Region

122eV Ce 4*f*→Resonance Maximum

114eV Ce 4*f*→Resonance Minimum

Ru 4*d*→Decrease in Cross Section

(Cooper Minima)

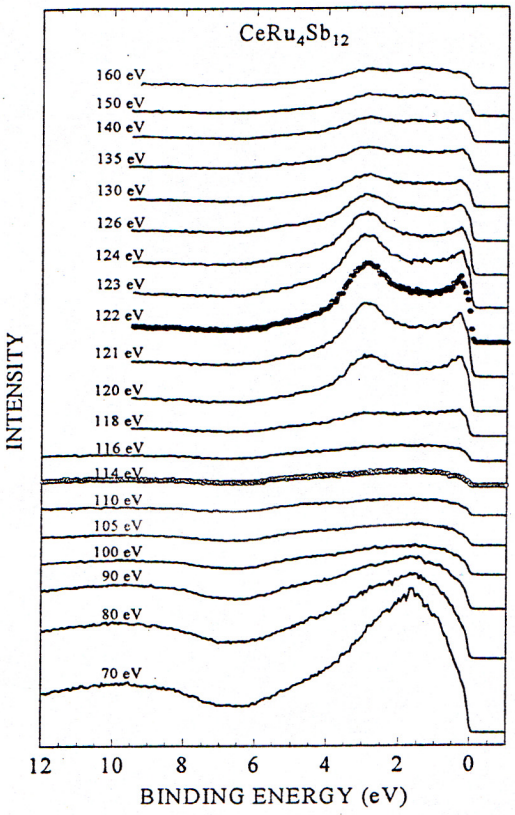

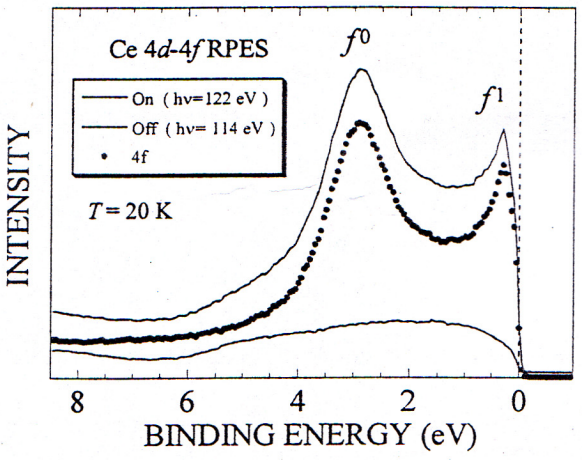

Ce 3*d*-4*f* Excitation

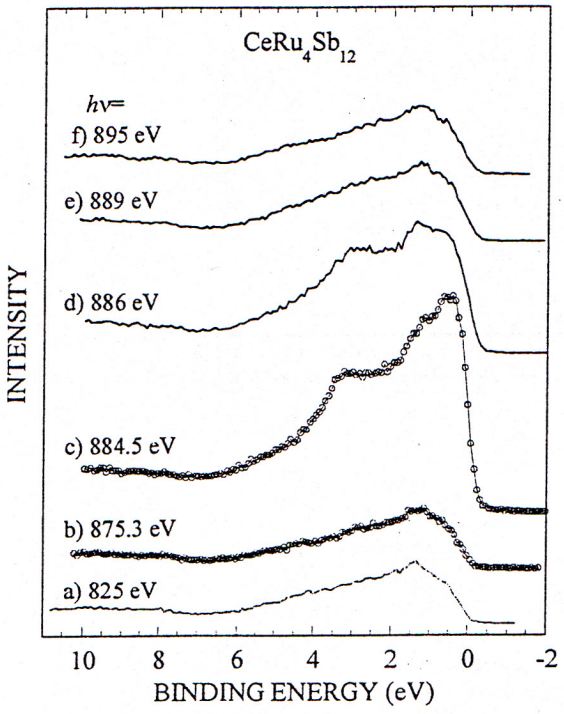

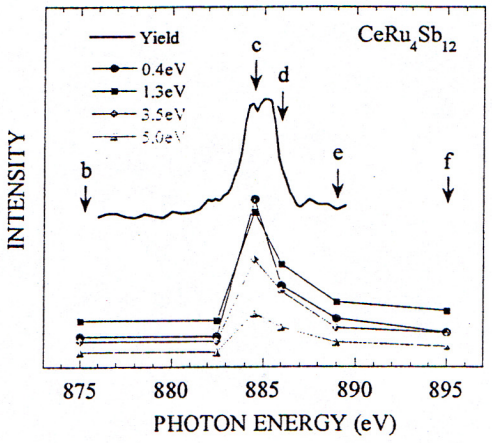

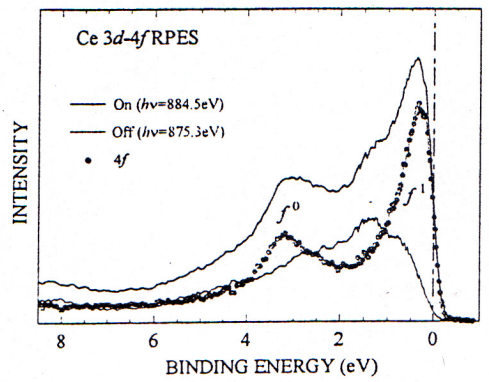

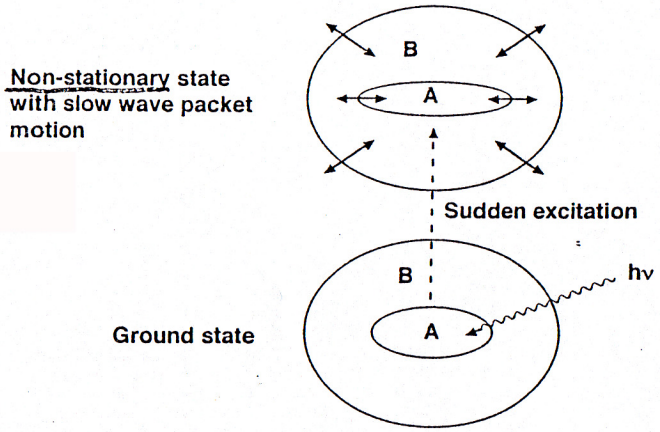

Sudden approximation

$\omega_{excit.} \gg \omega_{relax.}$

A system is decomposed into two parts.

Example:

(A) Photoelectron

(B) Other electrons & ions

Sudden approximation

$$\begin{cases} t<0 & H_0 \\ t\geq 0 & H = H_0 + V \end{cases}$$

eigenstates of H_0: $|U_n\rangle e^{i\omega_n t}$ $(n=1,2,\cdots)$

" of H: $|V_m\rangle e^{i\omega_m t}$ $(m=1,2,\cdots)$

i) $|U_m\rangle$ state at $t<0$

ii) continuity of wavefunction at $t=0$

$$|U_n\rangle = \sum_m b_m |V_m\rangle, \qquad b_m = \langle V_m | U_n\rangle, \quad b_m^* = \langle U_n | V_m\rangle$$

iii) for H_0 at $t>0$

$$|\Phi_0(t)\rangle = e^{i\omega_n t}|U_n\rangle \quad \text{——①}$$

for H at $t>0$

$$|\Phi(t)\rangle = \sum_m b_m e^{i\omega_m t}|V_m\rangle \quad \text{——②}$$

overlap integral of ① and ②

$$\begin{cases} g(t) \equiv \langle \Phi_0(t)|\Phi(t)\rangle = \sum_m e^{i(\omega_m-\omega_n)t}|b_m|^2 \\ \tilde{g}(t) \equiv \langle \Phi_0(0)|\Phi(t)\rangle = \sum_m e^{i\omega_m t}|b_m|^2 \end{cases}$$

$|b_m|^2$: Fourier coefficient of

$$\begin{cases} g(t) \\ \tilde{g}(t) \end{cases} \quad \text{for} \quad \begin{cases} \omega = \omega_{m-n} \\ \omega = \omega_m \end{cases}$$

Two descriptions of sudden approximation

$H_0 \rightarrow H_0 + V(t>0)$

1) Probability amplitude that the state remains the old state : $g(t)$ or $\tilde{g}(t)$

$|b_m|^2$: Fourier transform of $g(t)$ or $\tilde{g}(t)$

Relaxation

2) Expand the old state $|U_n\rangle$ in terms of the eigenstates $|V_m\rangle$ of H

b_m : expansion coefficient

Configuration interaction

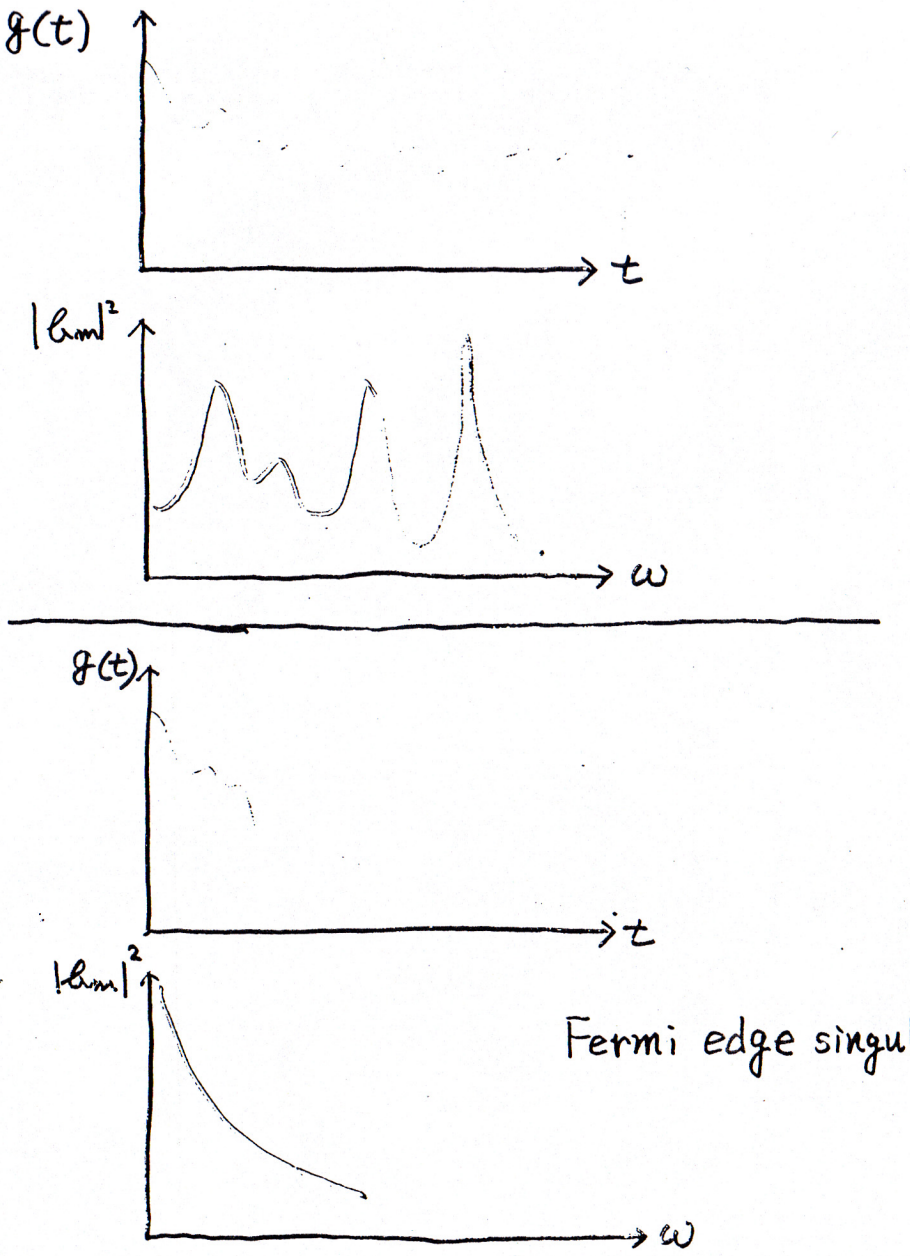

Fermi edge singularity

"Exciton effect" Metals and Semiconductor

1 Simple Metals. Na, K, Rb, Cs, Al, Mg

Manybody effect: MND theory

"Fermi edge singularity"

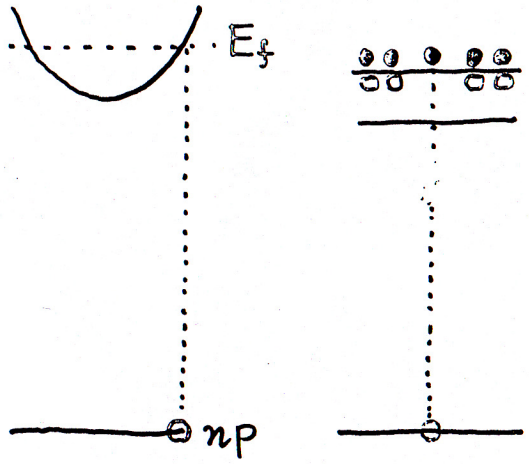

"Fast screening"

Long range potential

↓

short ..."

"Slow screening"

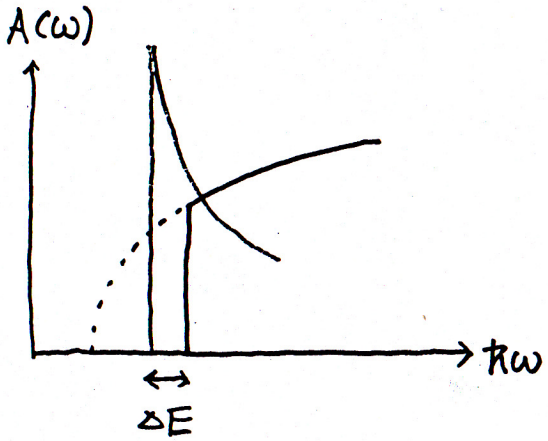

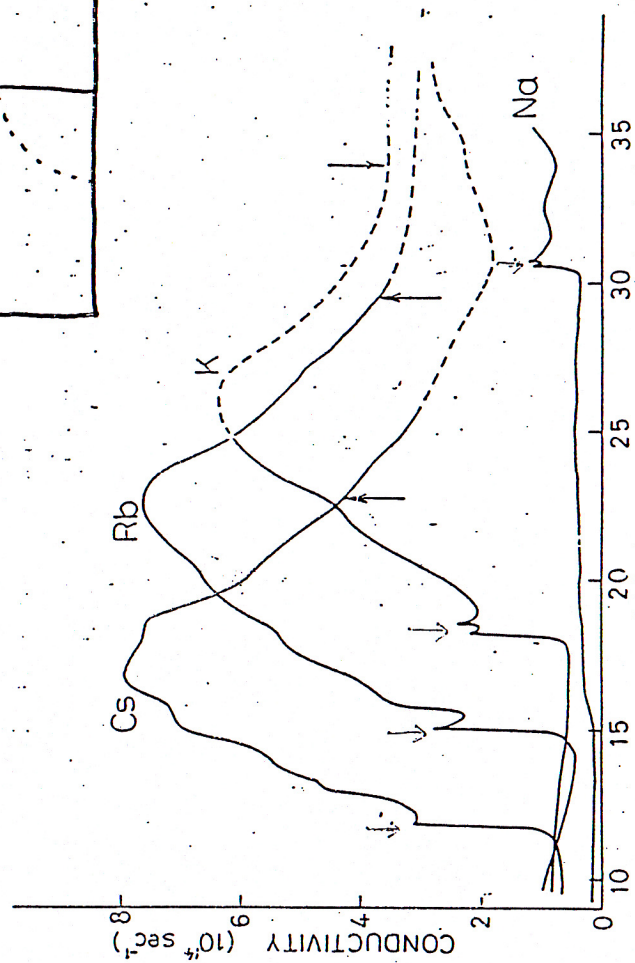

Fig. 2. Optical absorption spectra of Na, K, Rb and Cs. Full lines: measured with the apparatus connected to the 0.4 GeV storage ring (where the absolute values of the absorption coefficients were determined). Broken lines: measured with the apparatus connected to the 1.3 GeV synchrotron. Arrows: expected threshold of the s-shell absorption. Assumption is made that the refractive indices are unity.

Effect of core hole

1) increase in attractive potential

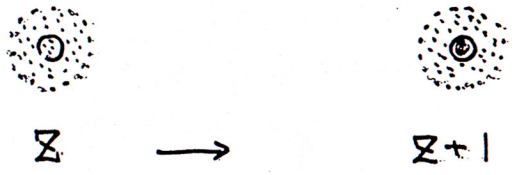

2) attractive force depends on the valence state

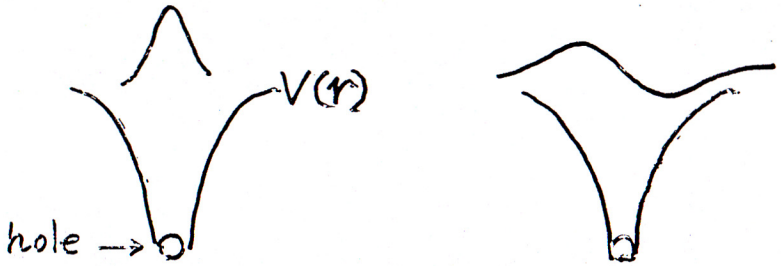

large force small force

3) some degrees of freedom (quantum numbers) of hole

(spin
  angular momentum

Coulomb int.
Exchang int. } between hole and other electrons

depends on the states → 2)

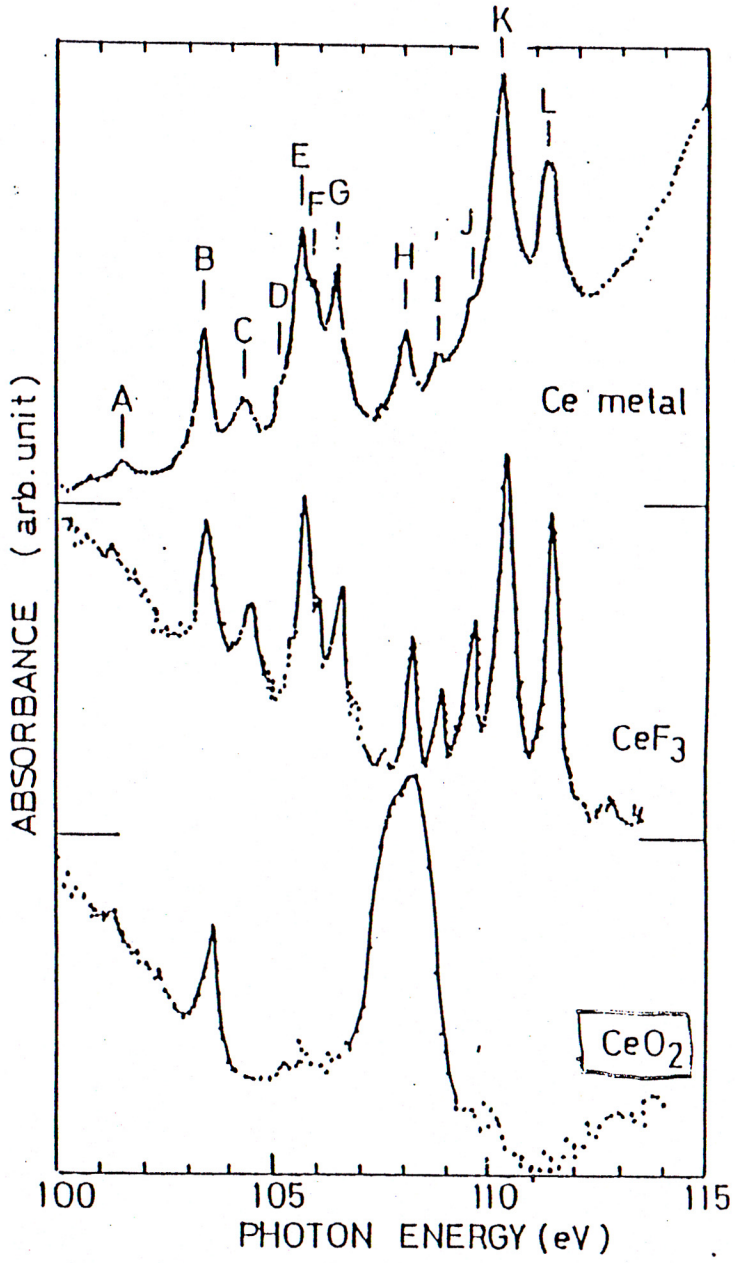

Fig. 1. The absorption spectra of cerium metal compounds in the region below the 4d abs cerium. The fine structures are indicated by A

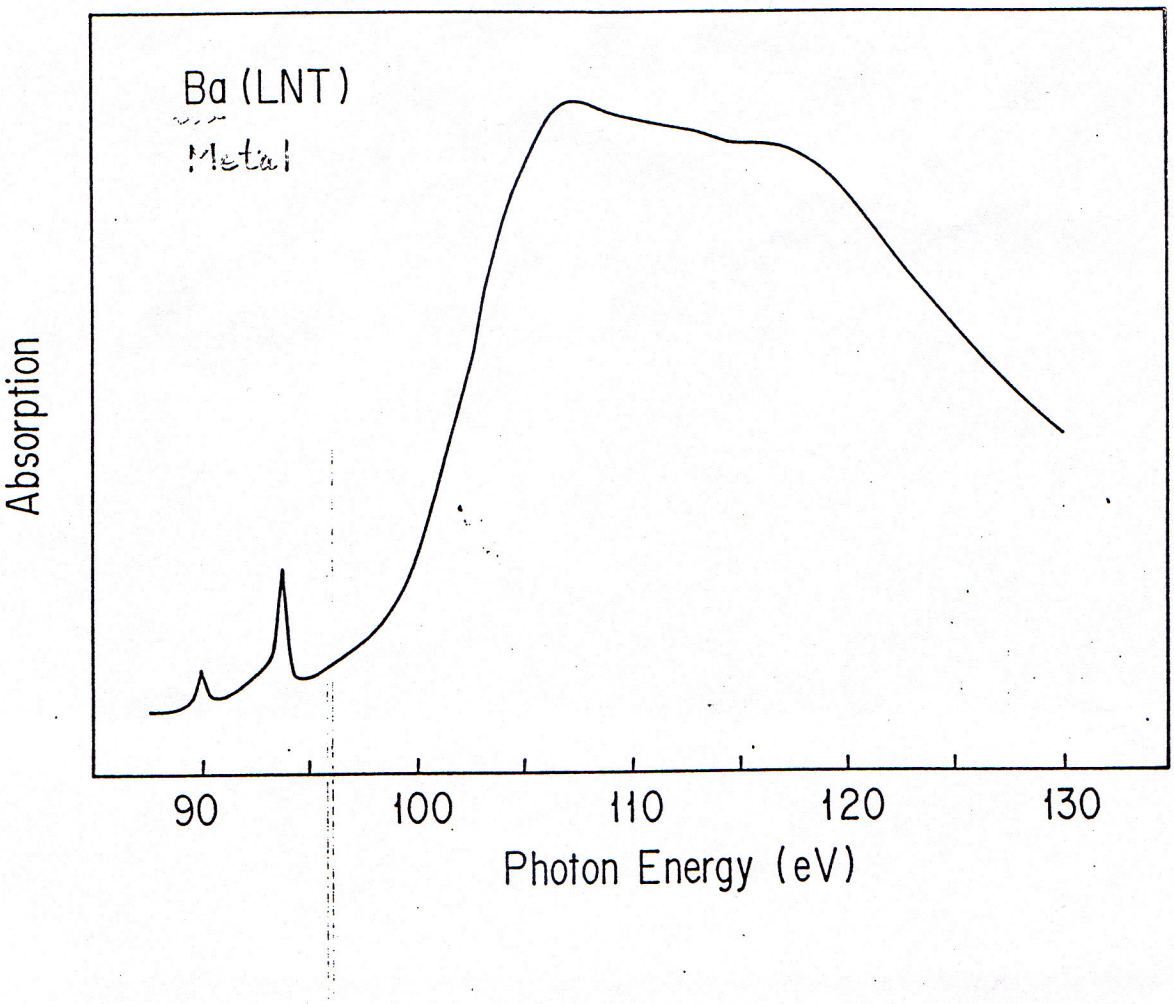
Ba (LNT)
Metal
Absorption
90
100
110
120
130
Photon Energy (eV)

Fig. 3 (a)

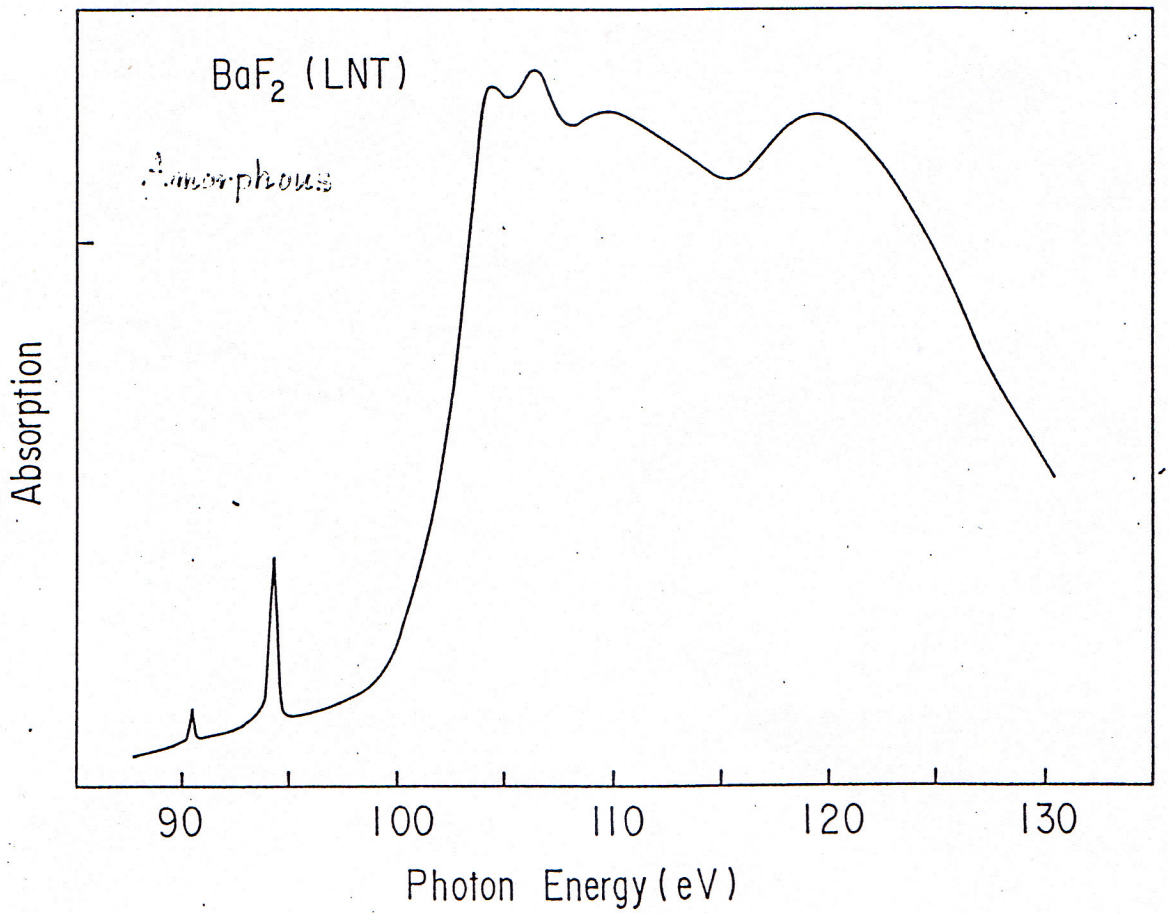
BaF2 (LNT)
Amorphous
Absorption
90
100
110
120
130
Photon Energy (eV)

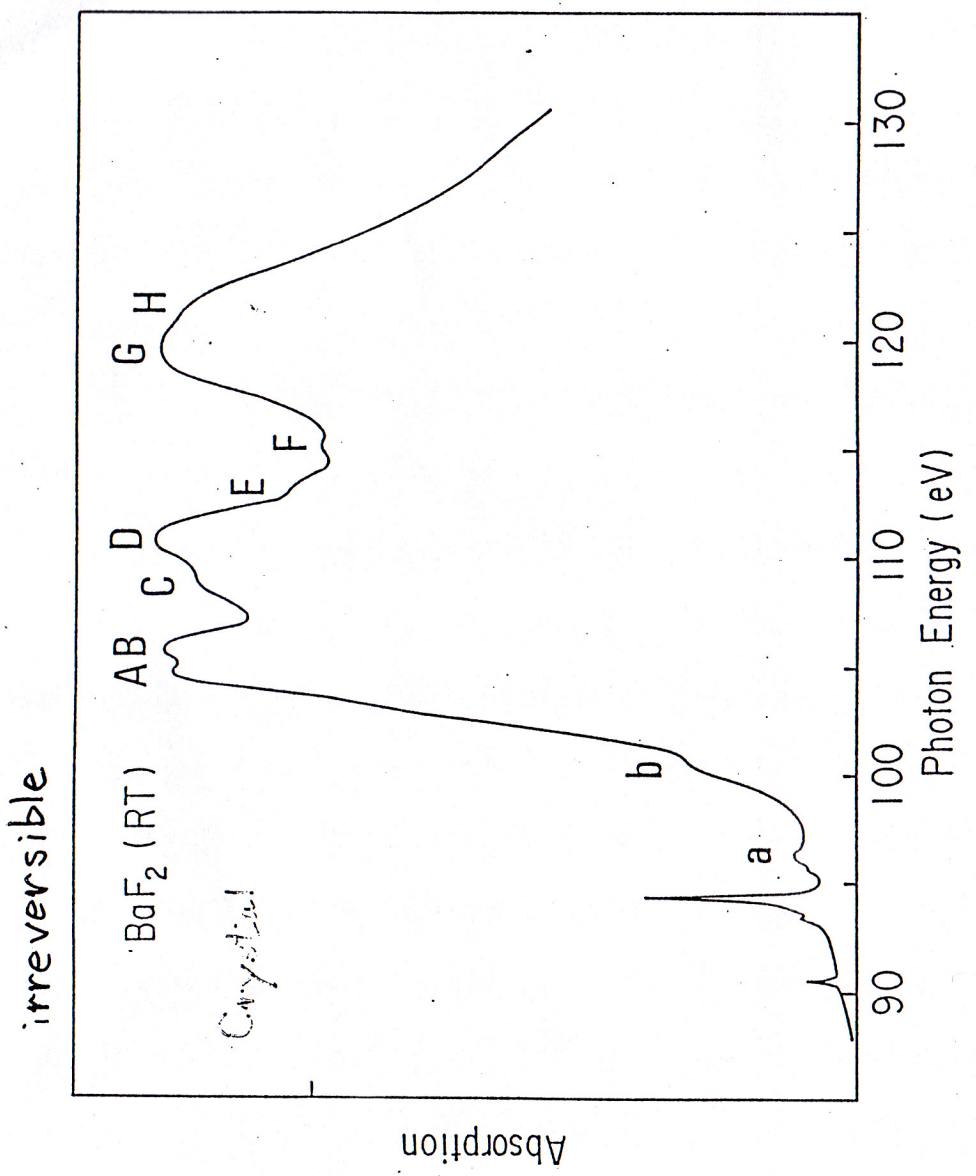

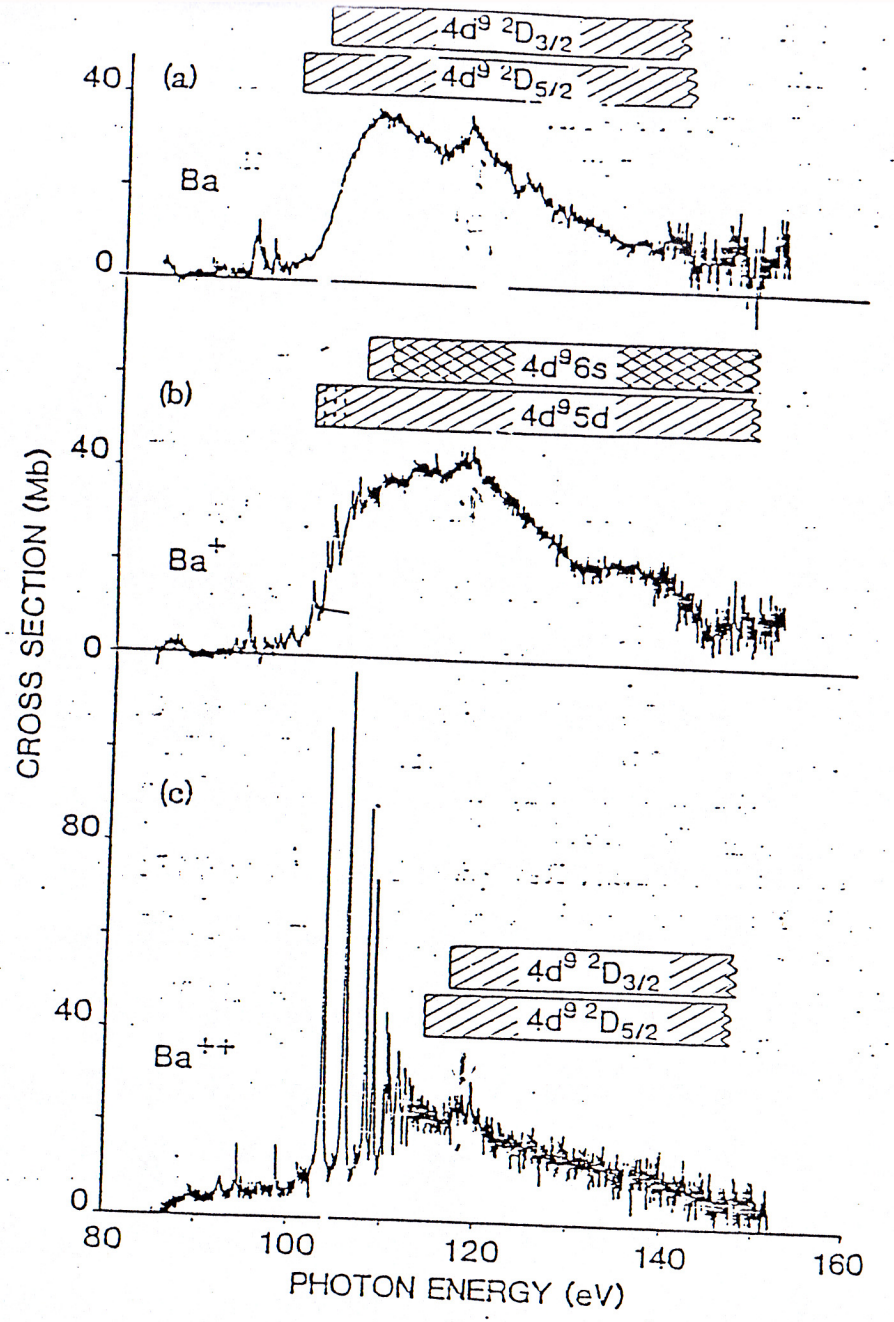

FIG. 1. Photoabsorption cross section of (a) Ba, (b) Ba^+, and (c) Ba^{++}. Peak cross sections of strong absorption features in Ba^{++} underestimated because of saturation and effects of limited resolution. Data obtained through calibration of photographic plates and

Magnetic circular dichroism (MCD)

μ^+ (μ^-): absorption with the photon spin parallel

(or anti-parallel) to the direction of the magnetic field

$\mu^+ - \mu^-$: MCD signal

Orbital sum rule(exact):

$$\langle L_z \rangle = \frac{I_1}{I_0} \mathrm{sgn}(l_1 - l_2) \max(l_1, l_2)$$

$$I_1 = \int (\mu^+ - \mu^-) \mathrm{d}\omega, I_0 = \int (\mu^+ + \mu^- + \mu^0) \mathrm{d}\omega$$

μ^0: absorption of photons linearly polarized *along z-axis*

Example: l_1=2 and l_2=3 for 2p-3d excitation

Spin sum rule (isotropic system, approximation)

2p-3d excitation

$$\frac{\langle S_z \rangle}{\langle L_z \rangle} = \frac{3\int_{L_3} (\mu^+ - \mu^-) \mathrm{d}\omega - 6\int_{L_2} (\mu^+ - \mu^-) \mathrm{d}\omega}{4\int_{L_2+L_3} (\mu^+ - \mu^-) \mathrm{d}\omega}$$

3d-4f excitation

$$\frac{\langle S_z \rangle}{\langle L_z \rangle} = \frac{\int_{M_5} (\mu^+ - \mu^-) \mathrm{d}\omega - \frac{3}{2}\int_{M_4} (\mu^+ - \mu^-) \mathrm{d}\omega}{2\int_{M_4+M_5} (\mu^+ - \mu^-) \mathrm{d}\omega}$$

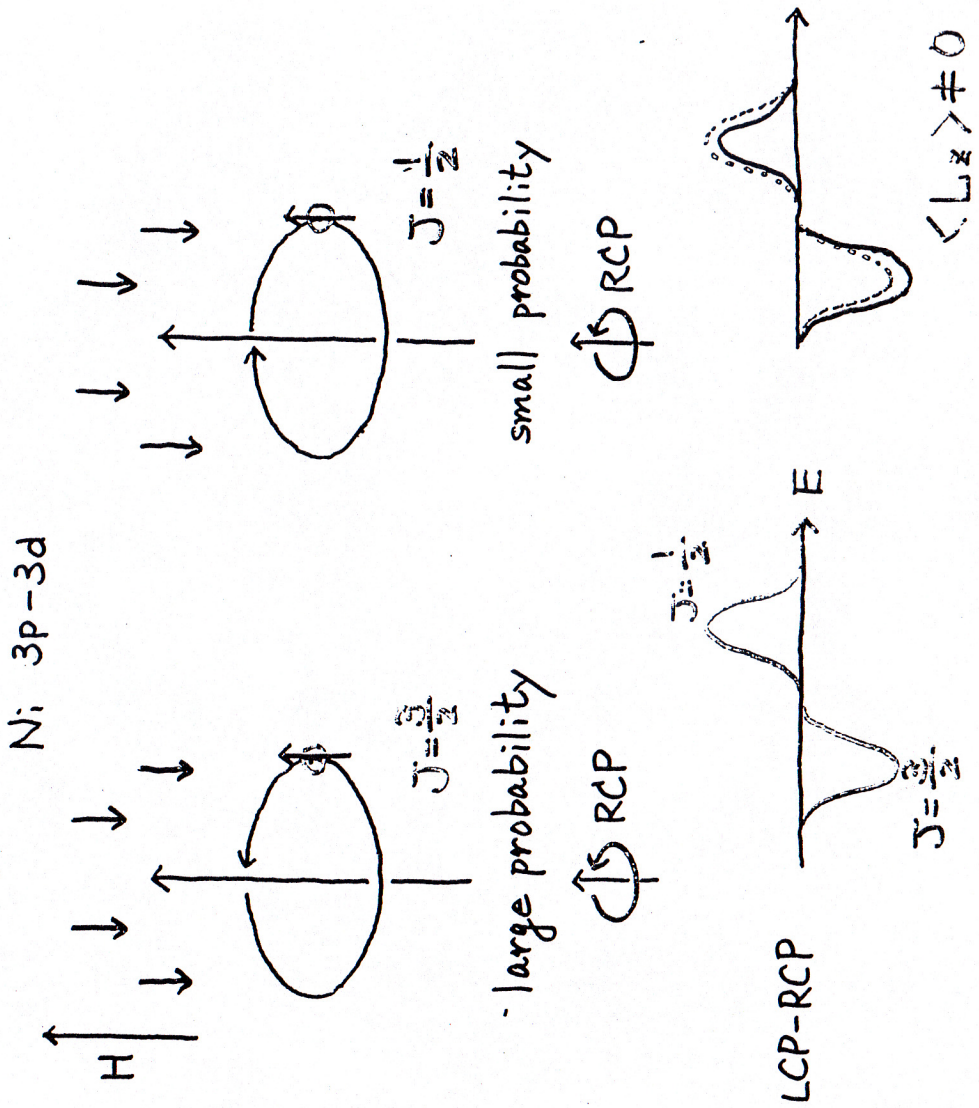

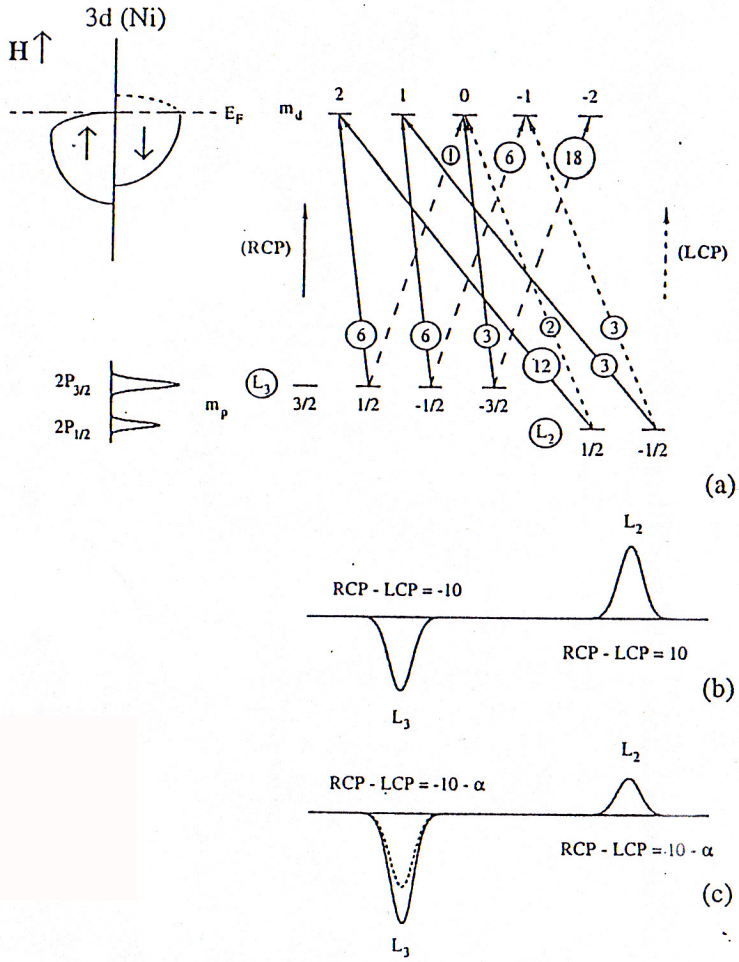

Figure 1.3. The m_d and σ_d dependence of the p→d transition probability for $2p_{3/2}$ and $2p_{1/2}$ in Ni are shown.

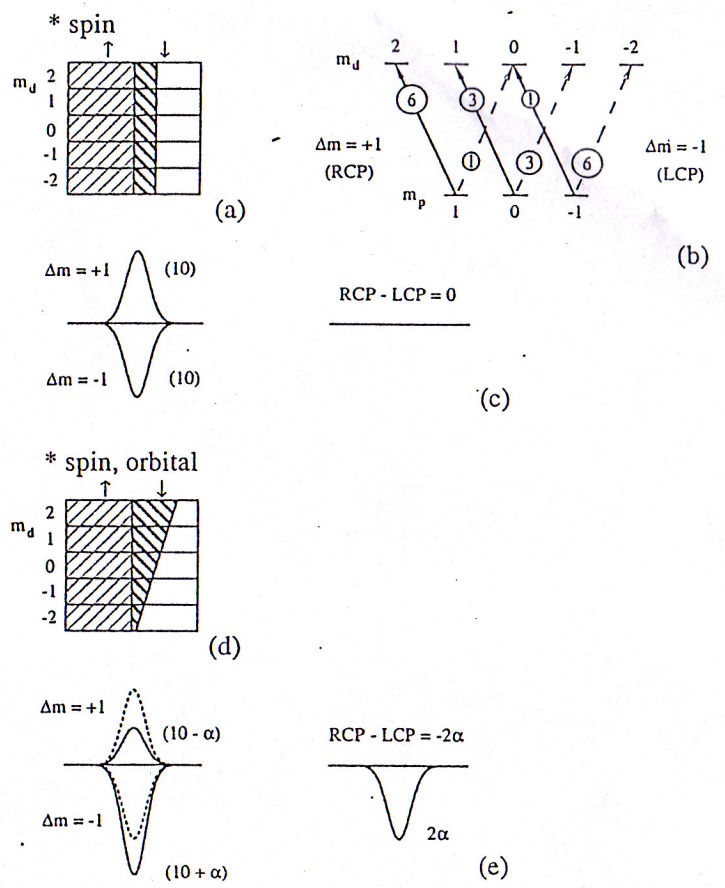

Figure 1.2. The MCD in the 2p→3d for 3d ferromagnets. Schematic illustration of occupied 3d states (shade area) specified by the 3d azimuthal quantum (m_d) and spin quantum numbers (σ_d) for the ferromagnetic states where only spin (a) and both spin and orbital moments (d) contribute to the magnetization. The m_d dependence of the p→d transition probability are shown in (b).

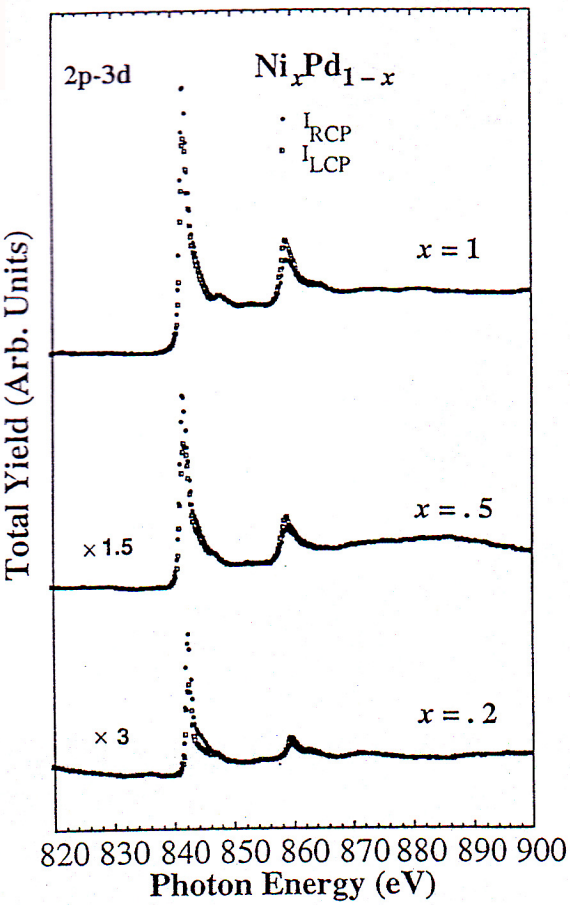
2p-3d
Ni_xPd_{1-x}
I_{RCP}
I_{LCP}
$x = 1$
$x = .5$
$x = .2$
× 1.5
× 3
Total Yield (Arb. Units)
820 830 840 850 860 870 880 890 900
Photon Energy (eV)

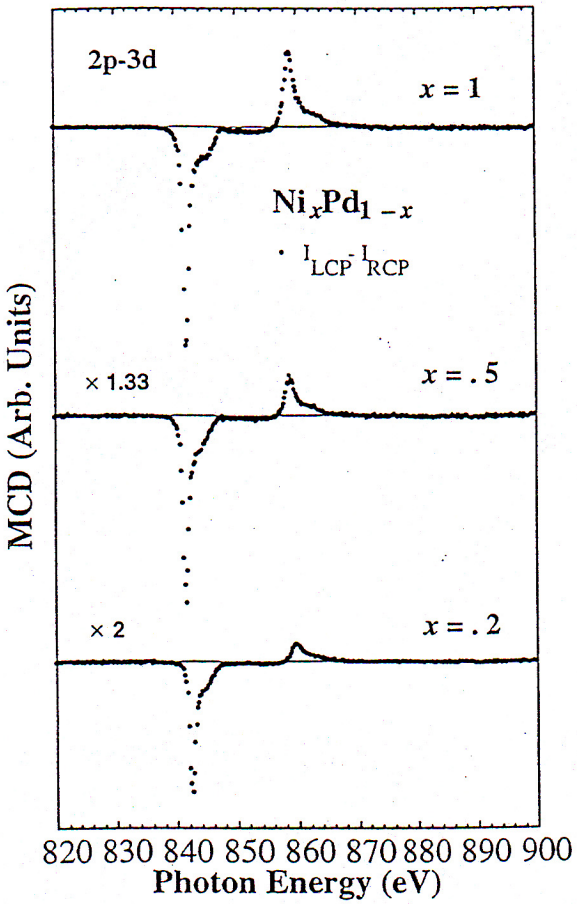
2p-3d
$x = 1$
Ni_xPd_{1-x}
I_{LCP}-I_{RCP}
× 1.33
$x = .5$
× 2
$x = .2$
MCD (Arb. Units)
820 830 840 850 860 870 880 890 900
Photon Energy (eV)

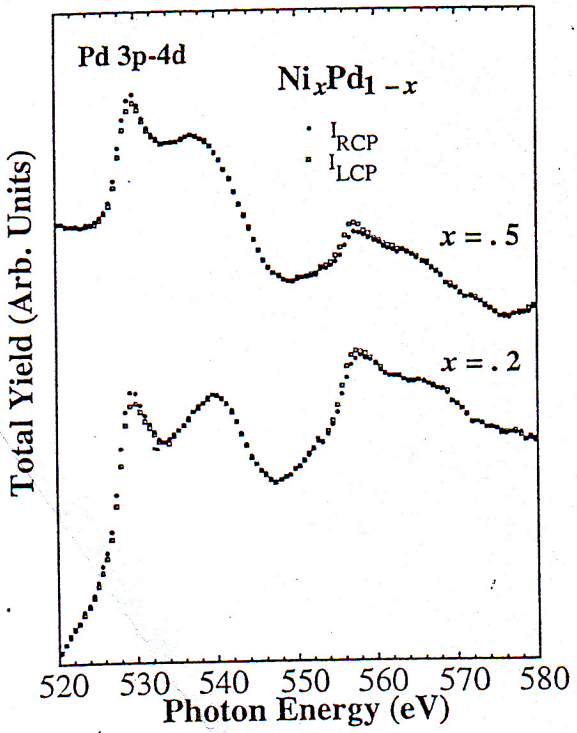
Pd 3p-4d
Ni_xPd_{1-x}
I_{RCP}
I_{LCP}
$x = .5$
$x = .2$
Total Yield (Arb. Units)
520 530 540 550 560 570 580
Photon Energy (eV)

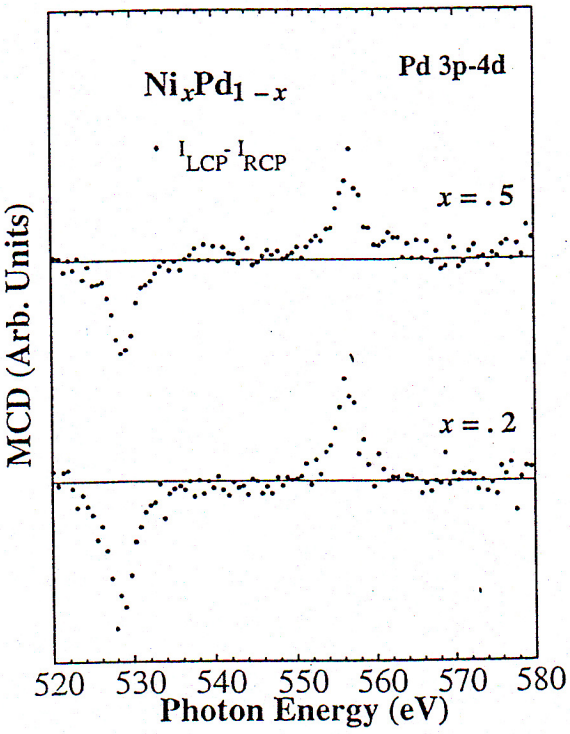
Ni_xPd_{1-x}
Pd 3p-4d
I_{LCP}-I_{RCP}
$x = .5$
$x = .2$
MCD (Arb. Units)
520 530 540 550 560 570 580
Photon Energy (eV)

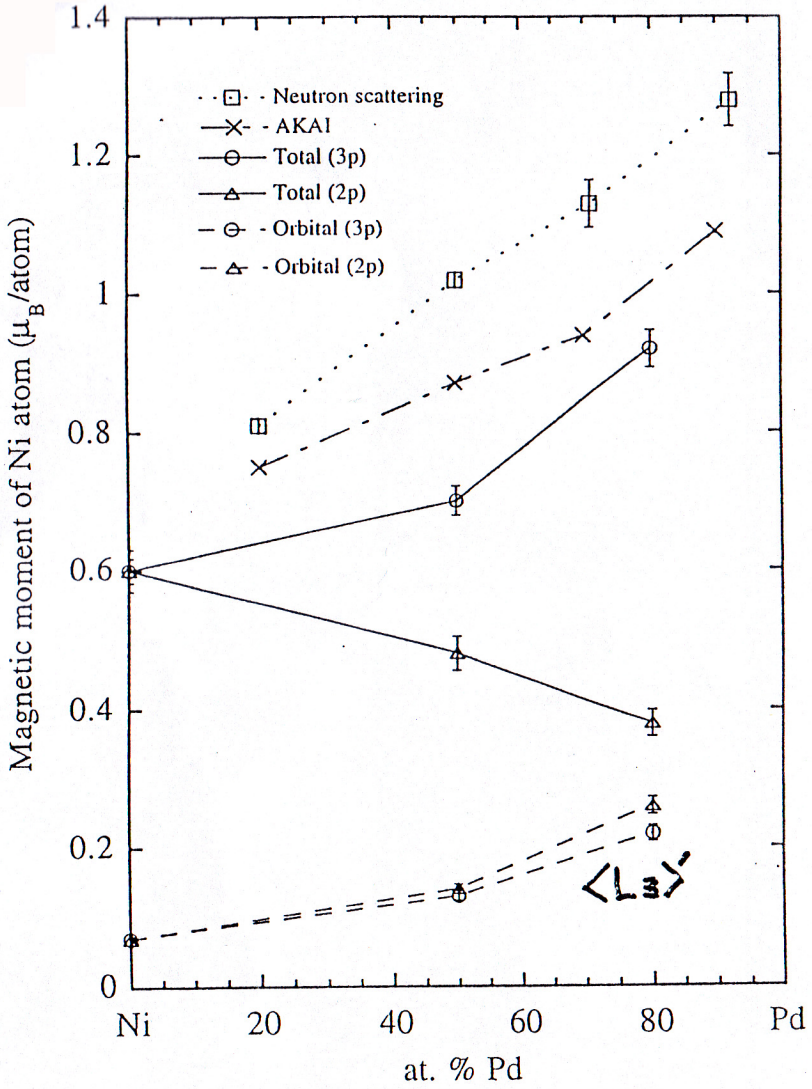
Neutron scattering
AKAI
Total (3p)
Total (2p)
Orbital (3p)
Orbital (2p)
Magnetic moment of Ni atom (μ_B/atom)
1.4
1.2
1
0.8
0.6
0.4
0.2
0
Ni
20
40
60
80
Pd
at. % Pd
<L3>'

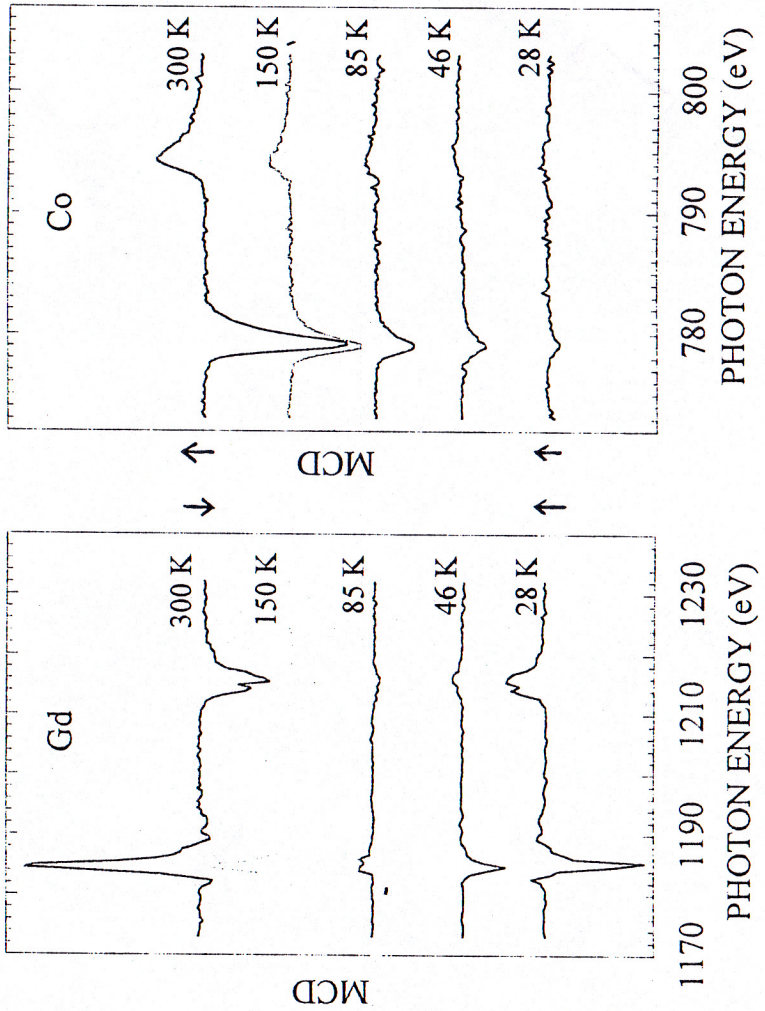
Co
300 K
150 K
85 K
46 K
28 K
780
790
800
PHOTON ENERGY (eV)
MCD
Gd
300 K
150 K
85 K
46 K
28 K
1170
1190
1210
1230
PHOTON ENERGY (eV)
MCD

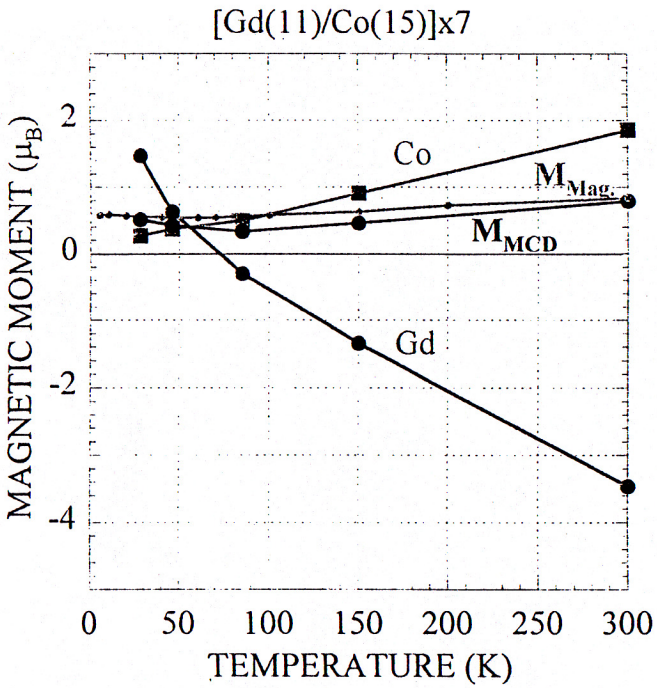

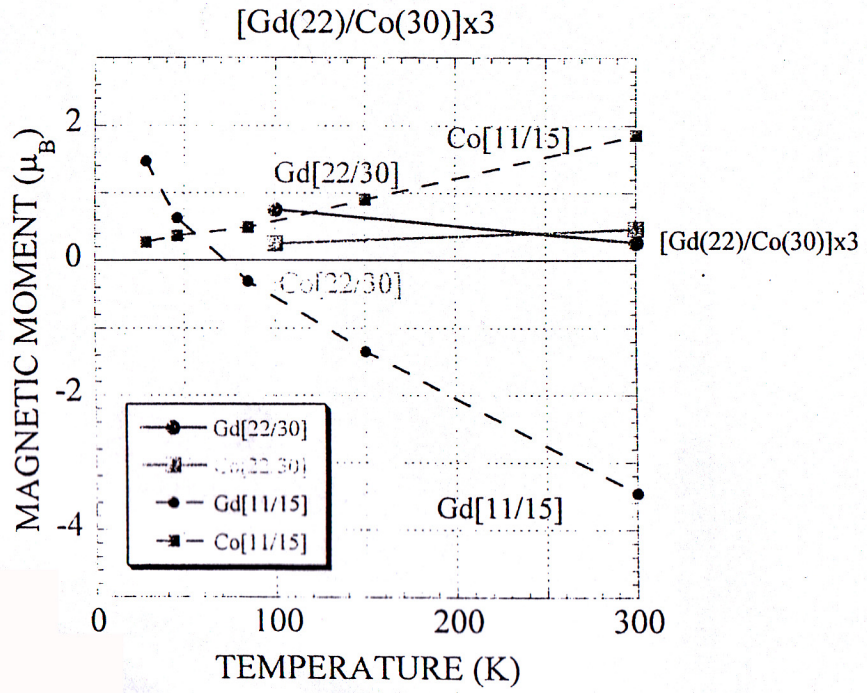

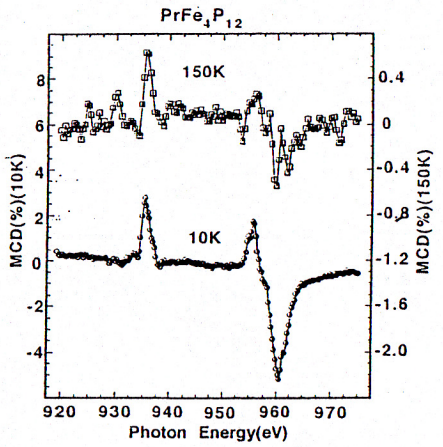

Fig. 1. MCD spectra of $PrFe_4P_{12}$ at 150 K and 10 K. μ^+ and μ^- mean that the spin of the incident photon is parallel and antiparallel, respectively, to the direction of the applied magnetic field. The MCD is defined as the difference $\mu^+ - \mu^-$.

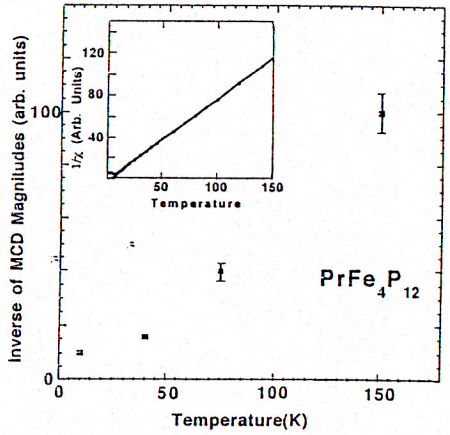

Fig. 2. The inverse values of the MCD magnitudes versus temperatures on $PrFe_4P_{12}$. The curve is very different from the results of the bulk susceptibility, behaving as if T_K is much higher than 10 K.

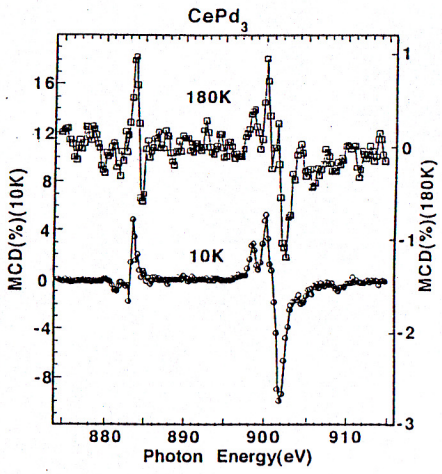

Fig. 3. MCD spectra of $CePd_3$ at 180 K and 10 K.

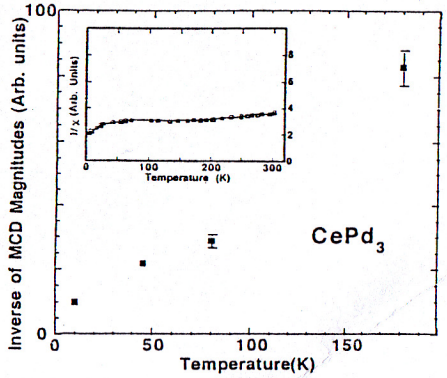

Fig. 4. The inverse values of the MCD magnitudes versus temperatures on $CePd_3$. The inverse values of the bulk susceptibility are inserted in the figure. The present four data points behave like a typical dilute Kondo alloy as if T_K is around 20 K, while the bulk transportation T_K is known to be around 150 K.